ChemPubSoc Europe

DOI: 10.1002/ejoc.201600349

EurJOC European Journal of Organic Chemistry

Full Paper

Julia Olefination

Development of a Modified Julia Olefination of Imides for the Synthesis of Alkaloids

Huu Vinh Trinh,[a] Lionel Perrin,*[b] Peter G. Goekjian,[a] and David Gueyrard*[a]

Abstract: We report the development of the intramolecular Julia olefination of imides. This original reaction produces *N*-fused bicyclic enamide compounds, which are interesting precursors in the synthesis of alkaloids. We show that this transformation enables access to [5,6], [6,5], and [6,6] fused bicyclic lactam enamides. The scope and the limitations of the reaction are presented as well as computational studies concerning novel mechanistic aspects of the title reaction.

Introduction

Fused bicyclic lactams and their synthesis have attracted considerable interest as a result of their ubiquity as frameworks in natural products; pyrrolizidine, quinolizidine and indolizidine alkaloids are all examples of such frameworks (Figure 1).[1,2]

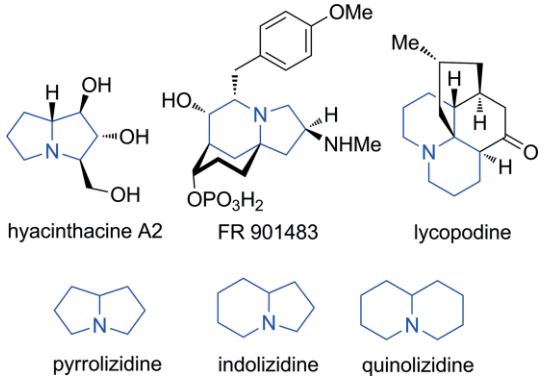

Figure 1. Bicyclic frameworks of alkaloid natural products.

New methodologies can provide new bond disconnections, and ultimately, new synthetic approaches to this broad family of natural products. Classical methods for the synthesis of bicyclic alkaloid skeletons generally create the C–N bond using: i) lactamisation,[3] ii) Mitsunobu chemistry,[4] iii) nucleophilic substitution approaches,[5] or iv) reductive amination (Figure 2, path a).[6] Alternatively, α,β-unsaturated bicyclic lactams have been formed by ring closing metathesis[7] or organometallic chemistry[8] (Figure 2, path c). A few methods for forming the more strategic *exendo* C–C bond[9] have been reported using radical anion cyclizations[10] (Figure 2, path b). Methods for the synthesis of bicyclic lactams specifically from imides include: i) reductive cyclization using samarium diiodide,[11] ii) photoinduced electron transfer,[12] iii) titanium-mediated cyclization,[13] or iv) electroreductive cyclization.[14] However, these syntheses either produce the hemiaminal or form the enamine C=C double bond under equilibrium conditions, generally leading to regioisomeric mixtures. New methodologies are still required to fully benefit from straightforward disconnections and to enable efficient access to this broad family of natural products.

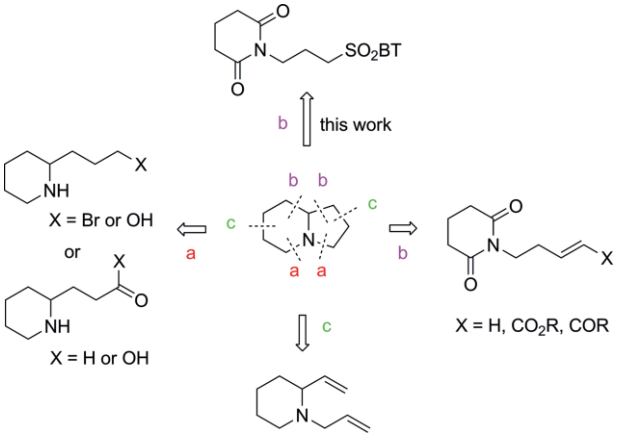

Figure 2. Principal disconnections of a bicyclic alkaloid framework.

We report herein a convenient and efficient synthesis of nitrogen-fused bicyclic lactam enamides using a modified Julia olefination of imides. This reaction allows the formation of the strategic *exendo* C–C bond[9] and provides a polyvalent enamide functional group for further elaboration.

The modified Julia olefination[15] is a useful method for the formation of C=C double bonds. In our effort to extend the scope of this reaction to other carbonyl functional groups, in

[a] *Laboratoire Chimie Organique 2 Glycochimie, Université de Lyon, ICBMS, UMR 5246 – CNRS, Bat. 308 – Curien (CPE Lyon), Université Claude Bernard Lyon 1, 43 Bd. du 11 Novembre 1918, 69622 Villeurbanne, France*
E-mail: david.gueyrard@univ-lyon1.fr
http://www.icbms.fr/co2glyco
[b] *Interface Theory/Experiment: Mechanism & Modeling (ITEMM), ICBMS, UMR 5246 – CNRS, Bat. 308 – Curien (CPE Lyon), Université Claude Bernard Lyon 1, 43 Bd. du 11 Novembre 1918, 69622 Villeurbanne, France*
E-mail: lionel.perrin@univ-lyon1.fr
http://www.icbms.fr/itemm
Supporting information for this article is available on the WWW under http://dx.doi.org/10.1002/ejoc.201600349.

particular to carboxylic acid derivatives, we previously applied the modified Julia olefination to the conversion of lactones to enol ethers.[16] Recently, we successfully applied this methodology to the synthesis of enamides from lactams.[17] The latter transformation requires the presence of an electron-withdrawing group on the nitrogen atom as well as a strong Lewis acid in order to facilitate the initial addition step. As relatively few examples of intramolecular modified Julia olefinations have been described,[18] we sought to apply this chemistry to imide olefinations as a way of accessing valuable bicyclic frameworks according to Figure 3.

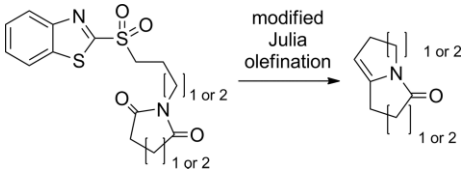

Figure 3. Intramolecular modified Julia olefination of imides.

The most similar approach to the one presented here was recently reported by Pohmakotr et al. using an intramolecular addition of a phenyl sulfoxide to an imide.[19] This synthetic sequence involves the nucleophilic addition of an α-sulfinyl carbanion, dehydration to the vinylsulfoxide, and reductive cleavage of the phenylsulfinyl group, to provide the analogous enamide lactam in a respectable 37 % overall yield. However, these conditions may not be compatible with certain total syntheses. Hence, the prospect of a direct access to cyclic enamides remains appealing.

Our approach extends the modified Julia olefination to the intramolecular reaction of imides. This work raises interesting mechanistic issues and is thus an opportunity to understand experimental results using DFT computational studies. Such studies were anticipated to render mechanistic insights into the intramolecular olefination of imides and ketones.

Results and Discussion

In the targeted intramolecular olefination (Figure 3), the use of an imide instead of a ketone or aldehyde is a significant change that can fundamentally alter the mechanism of the reaction; witness the differences between an aldol reaction and a Claisen condensation. Likewise, the intermediacy of a hemiaminal instead of an alcohol can be expected to significantly impact reaction pathways; such a difference provides an additional mechanism for *syn*–*anti* isomerization via the aminoketone.

Intramolecular Julia–Kocienski olefinations have been reported for the synthesis of cyclic alkenes.[18] In these cases, olefination involves an aldehyde and proceeds under mild conditions. The mechanism of the intermolecular Julia–Kocienski reaction has previously been scrutinized by DFT computational studies.[20,21] Vidari et al. pointed out that the spirocyclic structure characteristic of the Smiles transposition is not a minimum on the potential energy surface, but rather, a transition state.[20] Robiette et al. have reported the computational mechanistic study of the intermolecular modified Julia olefination of aromatic aldehydes.[21] In this study, the high selectivity for *E*-olefination was attributed to a *syn*-periplanar elimination of the *cisoid-syn*-sulfinate. A preliminary DFT study was performed in order to evaluate the mechanistic differences between: i) inter- and intramolecular olefinations of ketones, and ii) intramolecular olefinations of ketones and imides.[22]

Figure 4 presents the energy profile of the olefination reaction starting from deprotonated sulfone **I$_N$** and its 1,3-diketo analog (**I$_C$**) used as energy reference. The calculations were performed in the absence of an explicit counterion, being therefore most analogous to deprotonation by an amine base such as DBU. Starting from imide **I$_N$**, *syn*- and *anti*-additions of the carbanionic site to the carbonyl group are similar kinetically (**II$_{synN}$** and **II$_{antiN}$**, 11.8 and 10.9 kcal mol^{-1} respectively) and thermodynamically (**III$_{synN}$** and **III$_{antiN}$**, 5.8 and 7.3 kcal mol^{-1} respectively). However, only the *syn*-addition product **III$_{synN}$** efficiently undergoes the Smiles rearrangement, which proceeds with a very low energy barrier [transition state (TS) **IV$_N$**, 7.5 kcal mol^{-1} relative to **I$_N$**, 1.8 kcal mol^{-1} relative to **III$_{synN}$**]. The exergonicity of 26 kcal mol^{-1} is the driving force for this irreversible rearrangement. Thus, despite the endergonicity and the low reverse energy barriers associated with the addition, the Smiles rearrangement is kinetically favored over reversion for the *syn*-diastereomer. As the *cisoid*/*transoid* rotation is prevented by ring constraints, before and after the Smiles rearrangement, the intramolecular modified Julia olefination proceeds via a *syn*-periplanar elimination of the *cisoid* sulfonate derived from the **III$_{syn}$** addition product. From sulfinite **V$_N$**, elimination of BTO$^-$ and SO_2 is almost barrierless and is driven thermodynamically by a clear entropic contribution leading to an overall exergonicity of 47 kcal mol^{-1}. The elimination proceeds by an asynchronous E2 mechanism in which the C···OBT bond length is lengthened from 1.49 to 2.01 Å whereas the C–S bond length is merely elongated by 0.05 Å in TS **VI$_N$**.

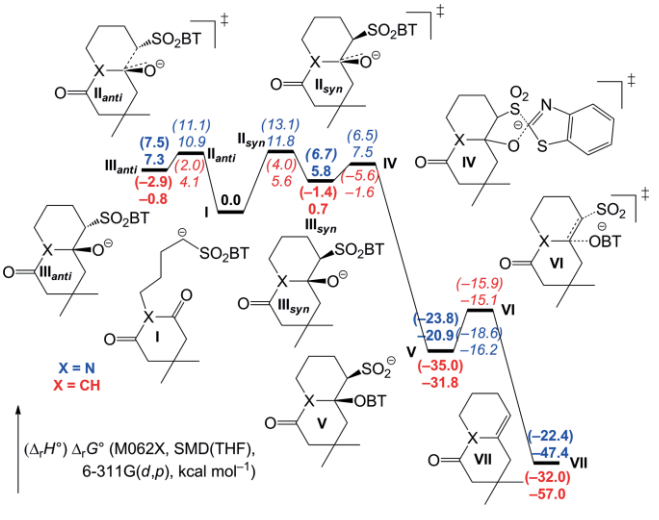

Figure 4. Enthalpy (in parentheses) and Gibbs energy profile for olefination of compound **2b** to yield **5** (blue), and its 1,3 diketo analog (red). For clarity, the *spiro* intermediate between **IV** and **V** has been omitted since its formation and subsequent evolution is not limiting.[23]

Comparison of the reactivity profile between imide **I$_N$** and its 1,3-diketo analog **I$_C$** reveals that the nitrogen atom significantly affects the addition step since the nucleophilic addition transi-

tion states are raised by approximately 6 kcal mol^{-1} in the nitrogen case, although the addition remains within a thermally accessible range. This is the expected manifestation of the lower electrophilicity of the imide group. The addition is also thermodynamically significantly more unfavorable in the case of the hemiaminal anion vs. the alkoxide. It is also worth noting that, in the 1,3-diketo analog, the computed energy barriers are lower than those previously reported.[20,21] This results both from the limited entropic contribution of the intramolecular reaction and the electrophilic activation induced by the homovicinal carbonyl group.

A second major difference between the two types of substrate appears at the elimination step. Whereas the energy barrier for the elimination of BTO$^-$ and SO_2 is low for imide $\mathbf{V_N}$ (4.7 kcal mol^{-1}), this barrier increases to 16.7 kcal mol^{-1} in carbon analog $\mathbf{V_C}$. This can be attributed to participation of the nitrogen atom in the cleavage of the C–OBT bond, via an asynchronous elimination transition state (vide supra). As a result, although the initial addition step is less favorable than in the ketone case, the elimination is expected to be faster. No inherent limitation is expected for the title variation of the Julia olefination, except for the unproductive *anti*-addition.

Experimentally, the intramolecular modified Julia olefination requires the preparation of heterocyclic sulfones linked to the imide by the nitrogen atom. The substrates were synthesized from the corresponding imides via a short and efficient sequence involving imide alkylation with a dibromoalkane,[24] followed by nucleophilic displacement of the terminal bromide with mercaptobenzothiazole and subsequent oxidation of the sulfur atom to furnish the heterocyclic sulfones on multigram scale (Scheme 1).[25]

Initial studies focused on the cyclization of substrate **2a** (Table 1, header). Attempted one-step olefination with DBU[18c] at room temperature gave no trace of cyclized products (Scheme 2). The reaction with KHMDS provided the desired product but in a poor 32 % yield, which nonetheless confirmed

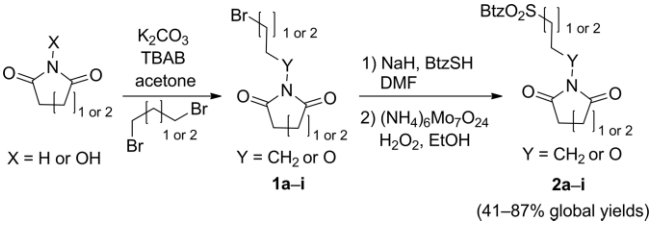

Scheme 1. General procedure for substrate synthesis.[26]

the calculated result that suggested the overall reaction pathway is energetically accessible from the anion. The use of LiHMDS under the same one-step Julia–Kocienski conditions failed to improve these results.

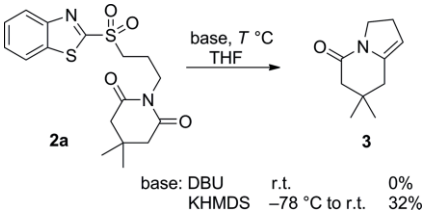

Scheme 2. One-pot intramolecular modified Julia olefination using imides under basic conditions.

Cyclization attempts using DBU at high temperature under thermal or microwave heating conditions led, instead, to an unprecedented radical fragmentation–substitution reaction of the benzothiazolyl sulfone with the THF solvent.[27] This side reaction was optimized using a radical initiator and diisopropylamine as base (Scheme 3).

Given the poor yields obtained with KHMDS, we investigated the conditions developed for lactones (Table 1).[16] The first step involved 2 equiv. of LiHMDS and 2 equiv. of boron trifluoride–diethyl ether at –78 °C for 1 h, followed by hydrolysis at low temperature and treatment of the crude intermediate with DBU

Table 1. Optimization of reaction conditions for the Smiles rearrangement–elimination step.

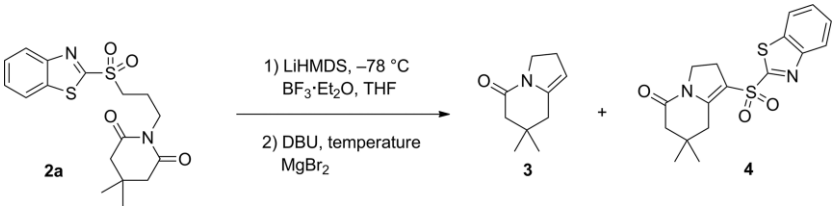

Entry	DBU (equiv.)	*T* [°C]	$MgBr_2$ (equiv.)	Yield of **3** [%]	Yield of **4** [%]
1	2	r.t.	0	70	n.d.
2	2.5	r.t.	0	79	11
3	4	r.t.	0	60	8
4	2.5	50	0	55	6
5	4	50	0	61	0
6	4	50	2	69	22
7	0	50	2	0	> 95[a]
8	0	r.t.	2	0	> 95[a]
9	0	50	0	0	45
10	0	r.t.	0	0	89

[a] Crude product was obtained in sufficient purity without chromatography (quantitative, yield > 95 %).

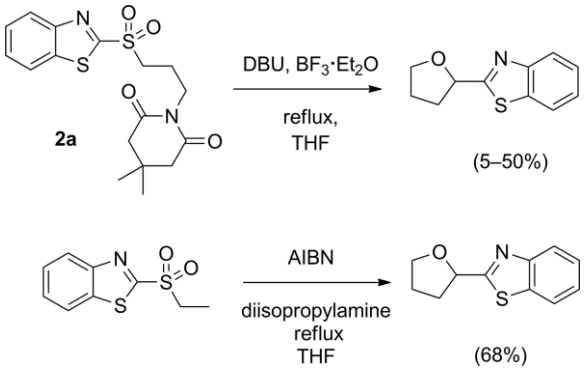

Scheme 3. Radical reaction between benzothiazolyl sulfone and THF at elevated temperatures.[28]

to provide enamide **3** and vinyl sulfone **4** (Table 1). We were gratified to obtain bicyclic enamide **3** in 70 % yield (Table 1, Entry 1).

Analysis of the crude intermediate reaction mixture showed complete formation of the expected hemiaminal intermediate with partial reversion to starting material **2a** and formation of small amounts of vinyl sulfone **4** during the DBU-mediated Smiles migration–elimination.

Further optimization of the second step was therefore carried out. The use of rigorously anhydrous DBU led to a slight, but meaningful improvement to 79 % yield, with no observed reversion to starting material (Table 1, Entry 2). As per the DFT calculations (Figure 3), after deprotonation of the isolated hemiaminal by DBU to give anion $\mathbf{III}_{syn}$ (Figure 4), the Smiles rearrangement is kinetically favored over reversion to starting material. However, we were unable to completely suppress the formation of vinyl sulfone. The use of a larger excess of DBU (4 equiv.) at room temperature did not increase the yield (Table 1, Entry 3), nor did an increase in temperature to 50 °C (Table 1, Entries 4 and 5). In an attempt to favor the Smiles rearrangement under Lewis acid conditions, magnesium bromide was added. We only observed that at 50 °C, the proportion of vinyl sulfone increased to 22 % (Table 1), Entry 6).

We then focused on the possibility of obtaining vinyl sulfone dehydration product **3** as the major product. We ran the reaction in the presence of $MgBr_2$ without DBU at 50 °C. In this case, the dehydration product was obtained in quantitative yield without purification (Table 1, Entry 7). We also showed that the reaction could be performed at room temperature (Table 1, Entry 8). Finally, we tried the reaction without added Lewis acid at 50 °C and at room temperature (Table 1, Entries 9 and 10, respectively). These reactions produced the desired product in 45 and 89 % yields, respectively, presumably due to the presence of trace acid. However, under these conditions the reaction was slower and the obtained product mixtures were less pure, thus necessitating a subsequent purification step. We were therefore able to obtain either bicyclic enamide **3** or the vinyl sulfone **4** in high yields depending on the conditions of the second step.

To assess the scope of the reaction, a panel of assorted sulfones were transformed into the corresponding enamides through modified Julia olefination under optimized conditions.[25] The results are compiled in Scheme 4. The enamides were generally obtained in moderate to good yields (55–80 %) except for the formation of [5,5]-fused bicyclic lactam **8**. In this particular case, the addition step did not occur, apparently due to the insolubility of deprotonated sulfones. DFT calculations reveal that the formation of the [5,5] pyrrolizidine framework is not kinetically prohibited although the formation of *syn*- and *anti*-hemiaminal intermediates are less favorable than for the homologous [6,5] indolizidine template (see Supporting Information). We also demonstrated that the reaction could be performed starting from *N*-hydroxysuccinimides and phthalimides (Scheme 4, compounds **10**–**12**, respectively).

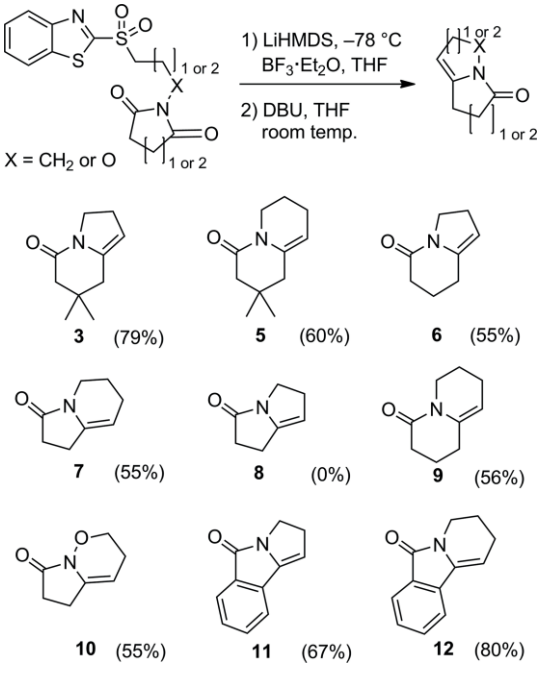

Scheme 4. Substrate scope of the modified Julia olefination.

Somewhat surprisingly, significant reversion to starting material was observed for the unsubstituted imides, leading to moderate yields (e.g. **6**, **7**, and **9**), which we were unable to overcome at this stage. In each case, there was no starting material remaining after the first step. Thus, these results were due to reversion during the elimination step, and not due to incomplete addition.

In order to obtain mechanistic information on the issue of reversion vs. elimination, we turned again to the application of DFT calculations with a focus on the effect of *gem*-dimethyl substitution (Table 2). Indeed, it is not immediately obvious why the unsubstituted cases **6** and **9** reproducibly give significant reversion (about 40 %) whereas little or no reversion is observed in *gem*-dimethyl-substituted analogs **3** and **5**.[29] Although one might be tempted to evoke a Thorpe–Ingold-type effect, there is no cyclization involving the imide ring in this reaction; steric arguments, on the other hand, would tend to favor the unsubstituted case. Based on the energy profile presented in Figure 4, two scenarios can be envisioned: i) dimethyl substitution either affects the relative energy of TSs $\mathbf{II}_{syn}$ and **IV** (kinetic effect on the relative rate of the transposition and

reversion), or ii) dimethyl substitution affects the relative amount of *anti*- over *syn*-hemiaminal, since the *anti*-hemiaminal does undergo Smiles transposition.

Table 2. Free energy data for the *syn*- and *anti*-addition to the carbonyl group of imide **I** and subsequent Smiles rearrangement that account for the synthesis of **3**, **5**, **6** and **9** ($\Delta_r G$ values in kcal mol^{-1} relative to **I**).

	[6,5]-scaffold		[6,6]-scaffold	
Lead compound	**3**	**6**	**5**	**9**
III$_{anti}$	9.7	7.3	7.3	6.9
TS-**II**$_{anti}$	12.7	12.9	10.9	11.2
TS-**II**$_{syn}$	14.2	14.5	11.8	10.5
III$_{syn}$	8.2	6.7	5.8	5.2
TS-**IV**	9.6	8.2	7.5	5.0
TS-**IV**-TS-**II**$_{syn}$	4.6	6.3	4.3	5.5

Starting from hemiaminal **III**$_{syn}$ involved in the synthesis of lead compounds **3**, **5**, **6** and **9**, the difference in energy between transition states **II**$_{syn}$ that account for the reversion, and transition states **IV** that account for olefination via the Smiles transposition is always computed in favor of the transposition by 4.3 to 6.3 kcal mol^{-1}. This difference in energy is sufficiently large that it cannot account for reversion to the starting material observed experimentally in the syntheses of **6** and **9**. If anything, the transposition is more strongly favored in the unsubstituted cases, as would be expected on the basis of steric arguments, although such small energy differences should not be overinterpreted. The use of the anion is reasonably representative of the conditions involving DBU as a base. Consequently, no support can be found for a more favorable reversion in the case of the unsubstituted compounds.

Alternatively, for this same set of compounds, the difference in energy between TSs **II**$_{anti}$ and **II**$_{syn}$ ranges from 0.7 to 1.6 kcal mol^{-1}. Thermodynamic stability is consistently in favor of *syn*-adduct **III**$_{syn}$. However, considering the precision of the computational method used,[30] further chemical interpretation of such differences is meaningless. As a result, the level of calculation used and/or the absence of Lewis acids in the chemical model is not able to capture the fine effects induced by the *gem*-dimethyl groups in **3** and **5** vs. **6** and **9**, respectively. Any computational support for such small energy differences (less than 1 kcal/mol) in such systems would be more misleading than informative, and the use of a purely qualitative rational model is therefore, more appropriate.

Both in situ FTIR results[27] and the high yields obtained by in situ elimination to the vinyl sulfone (vide infra) conclusively rule out incomplete addition in the unsubstituted cases **6** and **9**. No support, either computational or rational, can be found for a more favorable reversion in the unsubstituted cases. As a result, the remaining explanation is that *gem*-dimethyl cases **3** and **5** give predominantly the *syn*-hemiacetal in the addition step, whereas unsubstituted cases **6** and **9** provide a mixture of *syn*- and *anti*-hemiacetals; in the presence of DBU, the *syn*-hemiaminal will undergo Smiles rearrangement, whereas the *anti*-hemiaminal can lead only to the reversion product. It should be emphasized that, under traditional modified Julia conditions, the reaction is reversible, and the *syn*- and *anti*-intermediates are in equilibrium via the starting material. However, in the current case, we have shown that the starting material cannot access the hemiaminal form in the presence of DBU, and reversion will therefore be the endpoint of the reaction. A rational model for the effect of the *gem*-dimethyl group is presented in Figure 5. The antiperiplanar, Mukaiyama-like transition state is favored over the gauche transition state on the basis of stereoelectronic factors, but is disfavored by steric interactions due to the pseudo-axial orientation of the sulfone. Moreover, the presence of the *gem*-dimethyl group distorts the chair by repulsive interactions with the nascent axial C–O bond, thus increasing unfavorable steric interactions involving the sulfone.[31]

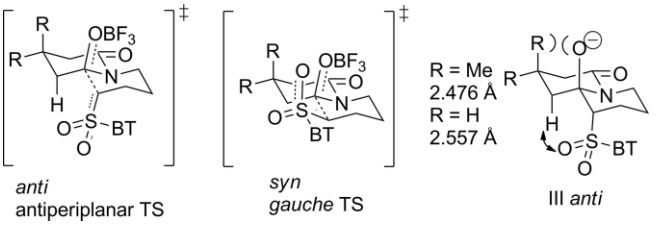

Figure 5. Rational model for the effect of the *gem*-dimethyl group on the stereoselectivity of the addition step. The lithium ion is not shown and the imide ring is drawn as a chair for the sake of clarity.

This interpretation is partially supported by the calculations and experimental results. The distance between the sulfoxide oxygen and the axial hydrogen is significantly shorter in the dimethyl case in the minimum energy conformation of the intermediate hemiaminal anion than in the unsubstituted case. As the transition state is expected to be late, these effects should also be observed in the transition state. In the ^{1}H NMR analysis of the hemiaminal obtained from **2a**, which was observed as a single isomer, Nuclear Overhauser effects support the assignment as *syn* (Figure 6). Although such effects with exchangeable hydroxyl protons are not definitive, the clean elimination also supports the assignment of the hemiaminal as the *syn*-isomer. Unfortunately, NMR experiments in the case of **3** were less conclusive, as significant elimination and reversion occurred prior to NMR analysis. In situ FTIR monitoring did not render any useful information pertaining to the diastereomeric mixtures.

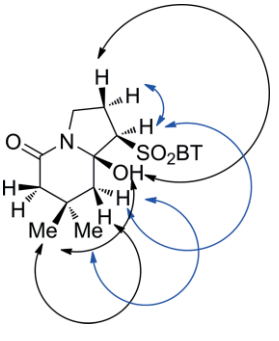

Figure 6. NOESY correlations observed for the intermediate hemiaminal.

We next turned our attention to the scope of the synthesis of vinyl sulfones (Scheme 5). The [5,6], [6,5] and [6,6] nitrogen-fused bicyclic vinyl sulfones were prepared in good yields. In a

manner similar to what was previously observed, the dimethylglutarimide gave a clean reaction, whereas the unsubstituted imides underwent significant reversion. Finally, when starting from succinimide, the process stopped at hemiaminal intermediates **19** and **20** and only a limited degree of elimination was observed in the case of vinylsulfone **18**. The elimination under Lewis acid conditions presumably occurs through a cationic E_1 mechanism. In order to account for these observations, we computed the following isodesmic reactions [see Equations (1), (2), and (3)] that account for the stability trend of intermediate carbocation $\mathbf{X}^+$ and final product **P** relative to hemiaminal $\mathbf{X_{OH}}$. In hemiaminal $\mathbf{X_{OH}}$, only the *syn*-isomer was considered.

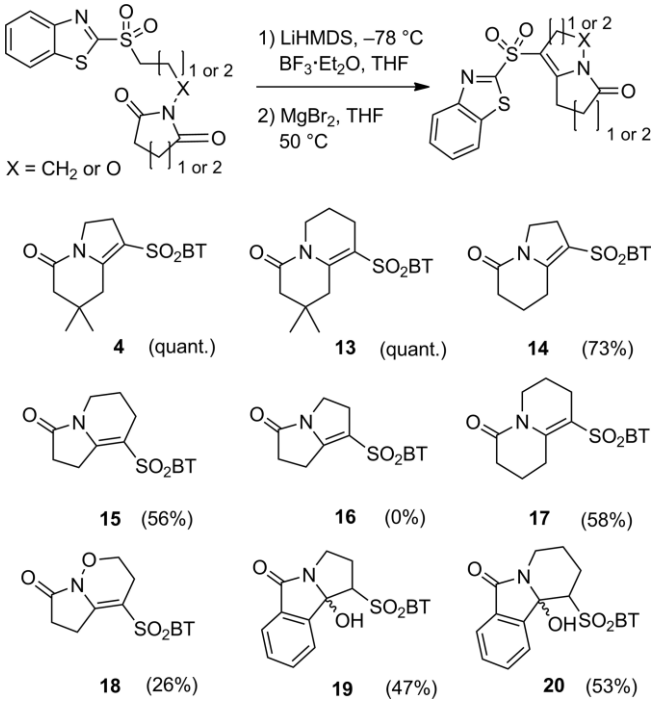

Scheme 5. Substrate scope for two-step vinyl sulfone synthesis.

$$\mathbf{X_{OH}}^{syn} + \mathbf{3} = \mathbf{3_{OH}}^{syn} + \mathbf{P} \quad (1)$$

$$\mathbf{X_{OH}}^{syn} + \mathbf{3}^+ = \mathbf{3_{OH}}^{syn} + \mathbf{X}^+ \quad (2)$$

$$\mathbf{X}^+ + \mathbf{3} = \mathbf{3}^+ + \mathbf{P} \quad (3)$$

Equation (1) conveys the overall thermodynamic trend to yield the vinylsulfone **P** from the hemiaminal $\mathbf{X_{OH}}$. For the set of molecules considered, this formal reaction is aergic (0 ± 3 kcal mol^{-1}). As a result, the lack of the stability of the vinylsulfones cannot be invoked. Equation (2) assesses the relative stability of putative iminium elimination intermediate $\mathbf{X}^+$. In this case, relative to scaffold $\mathbf{4}^+$, $\mathbf{13}^+$ is rigorously aergic, $\mathbf{18}^+$ is slightly endergonic by 1.2 kcal mol^{-1} and, $\mathbf{19}^+$ and $\mathbf{20}^+$ are clearly endergonic respectively by 7.2 and 4.4 kcal mol^{-1}. Finally, Equation (3) shows the thermodynamic trend of the final deprotonation. This step is thermodynamically favorable by at least 3 kcal mol^{-1}, relative to **4**, for all compounds. As a result, the limited yield observed for the formation of **18** and the absence of elimination in **19** and **20** is related to the instability of carbocation intermediate $\mathbf{X}^+$ generated by $MgBr_2$ abstraction of the hydroxy group.

As reversion to starting materials was also observed in the elimination step, we developed a one-pot procedure for the synthesis of vinyl sulfones by trapping the intermediate hemiaminal anion. At the end of the first step, the intermediate was treated in situ with two equivalents of acetyl chloride in order to induce the elimination (Scheme 6). We showed that this procedure is very effective in previously favorable cases such as **4**; it is even more effective for ordinarily less satisfactory cases such as those giving rise to **14**, **15** and **17**. Under the acetyl chloride-facilitated conditions **14**, **15** and **17** were generated in 91, 95 and 88 % yields, respectively. These results are consistent with the previous results, as the elimination is not expected to be stereospecific. These data also confirm that the observed starting material in the formation of the enamide is indeed due to reversion, and not to incomplete addition.

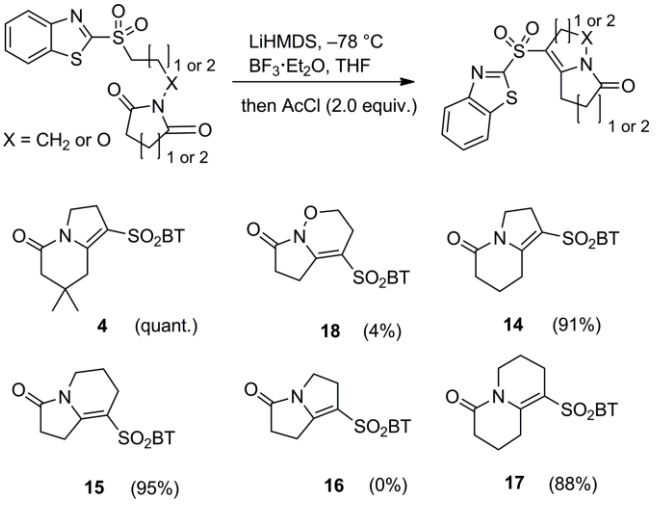

Scheme 6. In situ trapping procedure for the vinyl sulfone synthesis.

Nevertheless, in the particular cases of hydroxylsuccinimide **18** as well as the phthalamides **11** and **12**, the elimination step did not occur, because of the difficulty in forming the iminium intermediate, as supported previously by calculations. We circumvented this problem by using more forcing conditions that invoked mesylate formation and subsequent elimination under basic conditions. Vinyl sulfones **18**, **21** and **22** were thus obtained in moderate to good yields (47–71 %) (Scheme 7).

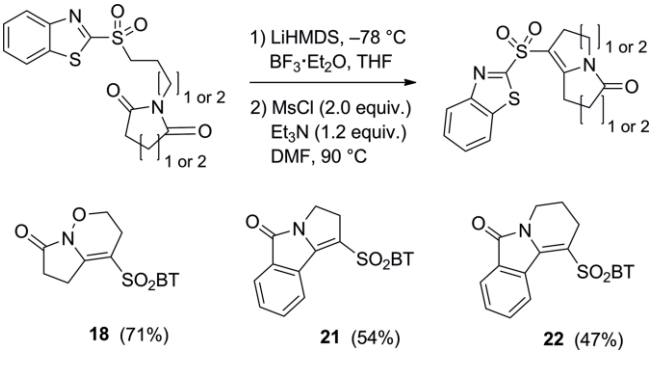

Scheme 7. Vinyl sulfone synthesis via mesylate formation.

Conclusions

We have developed a versatile method for the synthesis of nitrogen-fused bicyclic lactams bearing either enamide or vinylsulfone functional groups, using a modified Julia olefination of imides and dictated in part by the experimental conditions used during the second step. This transformation can provide an original route for the preparation of complex bicyclic alkaloids, and this work is actually under investigation. DFT calculations have shown that the initial addition step is significantly more demanding, both kinetically and thermodynamically, than in the case of ketone substrates, but that the elimination step is much faster. Only the *syn*-adduct can undergo Smiles rearrangement; the *anti*- adduct leads either to elimination affording the vinyl sulfone or to reversion to starting material.

Experimental Section

General: Experimental procedures for the preparation of compounds **2a**–**i** and the reactions in Scheme 3, spectroscopic data, and copies of the ^{1}H and ^{13}C NMR spectra of all reported compounds, as well as all calculated structures are available in the Supporting Information.

Unless otherwise noted, all experiments were carried out under argon. All solvents were distilled from the appropriate drying agents, purchased from Acros (seal bottle), or purified from Solvent Purification Systems from Innovative Technology. All reactions were monitored by thin layer chromatography (Macherey–Nagel). TLC plates were visualized by exposure to UV light or revealed using H_2SO_4 (10 %) in ethanol. All commercially available chemicals were used without further purification. Macherey–Nagel silica gel 60 (particle size 40–63 μm) was used for flash column chromatography. ^{1}H, ^{13}C NMR spectra were reported in ppm and were recorded with Avance Bruker (300 and 400 MHz) instruments in commercial $CDCl_3$ or [D_6]DMSO.

Typical Procedure for Enamides Synthesis: To a solution of 1-[3-(benzo[*d*]thiazol-2-ylsulfonyl)propyl]-4,4-dimethylpiperidine-2,6-dione (**1**) (300 mg, 0.79 mmol) in THF (24 mL) at –78 °C, was added boron trifluoride–diethyl ether (0.2 mL, 1.60 mmol) and lithium bis(trimethylsilyl)amide (1.0 M in toluene, 1.60 mL, 1.6 mmol). The mixture was stirred at –78 °C for 30 min. A phosphate buffer solution was added (3 mL) at –78 °C and the mixture was extracted three times with ethyl acetate. The combined organic layers were washed with brine, dried with Na_2SO_4 and the solvents evaporated under vacuum. The residue is dissolved in dry THF (24 mL) and DBU (0.3 mL, 2.01 mmol) was added. The mixture was stirred at room temperature for 10 min. A phosphate buffer solution was added (3 mL) at –78 °C and the mixture was extracted three times with ethyl acetate. The combined organic layers were washed with brine, dried with Na_2SO_4 and the solvents evaporated under vacuum. The crude product was chromatographed on silica gel using petroleum ether/EtOAc mixtures as eluent.

7,7-Dimethyl-2,6,7,8-tetrahydroindolizin-5(3*H*)-one (3): The crude product was chromatographed on silica gel using petroleum ether/EtOAc (2:3) as eluent to afford pure 7,7-dimethyl-2,6,7,8-tetrahydroindolizin-5(3*H*)-one **3** (105 mg, 79 %) as a colorless oil. ^{1}H NMR (300 MHz, $CDCl_3$): δ = 4.87 (br. s, 1 H), 3.82 (t, *J* = 8.5 Hz, 2 H), 2.58–2.49 (m, 2 H), 2.20 (s, 4 H), 0.95 (s, 6 H) ppm. ^{13}C NMR (75 MHz, $CDCl_3$): δ = 166.7, 139.0, 106.1, 45.8, 44.2, 36.8, 30.4, 27.7, 27.1 ppm. IR: $\tilde{\nu}_{max}$ = 2956, 2931, 2896, 2871, 1722, 1667, 1435, 1391, 1353, 1270, 1247, 1018 cm^{-1}. HRMS (ESI) calcd. for [M + Na]$^+$: $C_{10}H_{15}NNaO$ 188.1046, found 188.1041.

2,2-Dimethyl-1,2,3,6,7,8-hexahydro-4*H*-quinolizin-4-one (5): The crude product was chromatographed twice on silica gel using petroleum ether/ethyl acetate (4:6) as eluent to afford pure compound **5** (86 mg, 60 %) as a colorless oil. ^{1}H NMR (300 MHz, $CDCl_3$): δ = 4.73 (br. s, 1 H), 3.75–3.67 (m, 2 H), 2.29 (s, 2 H), 2.16 (s, 2 H), 2.09–2.00 (m, 2 H), 1.77 (m, 2 H), 0.96 (s, 6 H) ppm. ^{13}C NMR (75 MHz, $CDCl_3$): δ = 168.1, 134.3, 105.3, 46. 7, 43.4, 40.3, 29.2, 27.6, 22.5, 21.7 ppm. IR: $\tilde{\nu}_{max}$ = 2953, 2933, 2893, 2869, 1705, 1676, 1469, 1376, 1263, 1253, 1166, 750, 619 cm^{-1}. HRMS (ESI) calcd. for [M + Na]$^+$: $C_{11}H_{17}NNaO$ 202.1202, found 202.1199.

2,6,7,8-Tetrahydroindolizin-5(3*H*)-one (6): The crude product was chromatographed on silica gel using petroleum ether/ethyl acetate (4:6) as eluent to afford pure compound **6** (20 mg, 55 %) as a colorless oil. ^{1}H NMR (300 MHz, $CDCl_3$): δ = 4.83 (br. s, 1 H), 3.83 (t, *J* = 8.7 Hz, 2 H), 2.56–2.47 (m, 2 H), 2.46–2.35 (m, 4 H), 1.77 (m, 2 H) ppm. ^{13}C NMR (75 MHz, $CDCl_3$): δ = 167.3, 139.7, 104.8, 44.5, 32.1, 26.8, 23.3, 19.9 ppm. IR: $\tilde{\nu}_{max}$ = 2950, 2933, 2869, 1691, 1636, 1439, 1407, 1276, 1236, 1247, 1147 cm^{-1}. HRMS (ESI) calcd. for [M + H]$^+$: $C_8H_{12}NO$ 138.0913, found 138.0907.

1,5,6,7-Tetrahydroindolizin-3(2*H*)-one (7): The crude product was chromatographed on silica gel using petroleum ether/ethyl acetate (5:5) as eluent to afford pure compound **7** (59 mg, 55 %) as a colorless oil. ^{1}H NMR (300 MHz, $CDCl_3$): δ = 4.67 (br. s, 1 H), 3.47 (m, 2 H), 2.63–2.53 (m, 2 H), 2.45–2.36 (m, 2 H), 2.09–2.01 (m, 2 H), 1.72 (m, 2 H) ppm. ^{13}C NMR (75 MHz, $CDCl_3$): δ = 174.5, 138.2, 97.7, 39.0, 29.2, 22.6, 21.4, 20.5 ppm. IR: $\tilde{\nu}_{max}$ = 2933, 2871, 2849, 1700, 1660, 1652, 1446, 1409, 1330, 1278, 1204, 1150 cm^{-1}. HRMS (ESI) calcd. for [M + H]$^+$: $C_8H_{12}NO$ 138.0913, found 138.0910.

1,2,3,6,7,8-Hexahydro-4*H*-quinolizin-4-one (9): The crude product was chromatographed on silica gel using petroleum ether/ethyl acetate (6:4) as eluent to afford pure compound **9** (22 mg, 55 %) as a colorless oil. ^{1}H NMR (300 MHz, $CDCl_3$): δ = 4.71 (br. s, 1 H), 3.74–3.68 (m, 2 H), 2.49 (t, *J* = 6.5 Hz, 2 H), 2.40–2.32 (m, 2 H), 2.08–1.99 (m, 2 H), 1.76 (m, 4 H) ppm. ^{13}C NMR (75 MHz, $CDCl_3$): δ = 168.4, 135.6, 103.9, 40.3, 33.3, 30.0, 22.4, 21.7, 20.1 ppm. IR: $\tilde{\nu}_{max}$ = 2944, 2932, 2874, 2842, 1675, 1637, 1425, 1373, 1260, 1247, 1170, 773 cm^{-1}. HRMS (ESI) calcd. for [M + H]$^+$: $C_9H_{14}NO$ 152.1070, found 152.1073.

2,3,5,6-Tetrahydro-7*H*-pyrrolo[1,2-*b*][1,2]oxazin-7-one (10): The crude product was chromatographed on silica gel using petroleum ether/ethyl acetate (5:5) as eluent to afford pure compound **10** (22 mg, 55 %) as a colorless oil. ^{1}H NMR (300 MHz, $CDCl_3$): δ = 4.83 (br. s, 1 H), 4.19 (t, *J* = 5.2 Hz, 2 H), 2.71–2.60 (m, 2 H), 2.50–2.40 (m, 2 H), 2.33–2.26 (m, 2 H) ppm. ^{13}C NMR (75 MHz, $CDCl_3$): δ = 165.9, 134.7, 94.3, 69.3, 26.3, 22.4, 20.1 ppm. IR: $\tilde{\nu}_{max}$ = 2983, 2936, 2876, 1722, 1685, 1637, 1371, 1363, 1326, 1240, 1060, 1046, 942, 913, 726 cm^{-1}. HRMS (ESI) calcd. for [M + Na]$^+$: $C_7H_9NNaO_2$ 165.0525, found 162.0521.

2,3-Dihydro-5*H*-pyrrolo[2,1-*a*]isoindol-5-one (11): The crude product was chromatographed on silica gel using petroleum ether/ethyl acetate (6:4) as eluent to afford pure compound **11** (90 mg, 67 %) as a colorless oil. ^{1}H NMR (300 MHz, $CDCl_3$): δ = 7.79 (d, *J* = 7.5 Hz, 1 H), 7.61 (d, *J* = 7.1 Hz, 1 H), 7.45 (m, 2 H), 5.72 (t, *J* = 3.0 Hz, 1 H), 3.89 (t, *J* = 7.7 Hz, 2 H), 3.16 (td, *J* = 7.8, 3.0 Hz, 2 H) ppm. ^{13}C NMR (75 MHz, $CDCl_3$): δ = 162.9, 141.8, 136.6, 130.8, 130.3, 129.3, 123.2, 121.6, 106.0, 40.0, 34.9 ppm. IR: $\tilde{\nu}_{max}$ = 2957, 1771, 1704, 1467, 1440, 1494, 1366, 1236 cm^{-1}. HRMS (ESI) calcd. for [M + Na]$^+$: $C_{11}H_9NNaO$ 194.0576, found 194.0570.

3,4-Dihydropyrido[2,1-*a*]isoindol-6(2*H*)-one (12): The crude product was chromatographed on silica gel using petroleum ether/ethyl acetate (5:5) as eluent to afford pure compound **12** (116 mg, 80 %) as a colorless oil. ^{1}H NMR (300 MHz, $CDCl_3$): δ = 7.74 (d, J = 7.4 Hz, 1 H), 7.52 (d, J = 7.5 Hz, 1 H), 7.44 (t, J = 7.0 Hz, 1 H), 7.36 (t, J = 7.1 Hz, 1 H), 5.76 (t, J = 4.5 Hz, 1 H), 3.73 (t, J = 5.9 Hz, 2 H), 2.32 (m, 2 H), 1.90 (m, 2 H) ppm. ^{13}C NMR (75 MHz, $CDCl_3$): δ = 165.6, 135.0, 134.7, 131.2, 129.8, 128.6, 122.7, 119.3, 104.7, 38.2, 22.2, 21.4 ppm. IR: $\tilde{\nu}_{max}$ = 2935, 2865, 2842, 1734, 1693, 1664, 1471, 1468, 1403, 1359, 1237, 725, 717, 692 cm^{-1}. HRMS (ESI) calcd. for $[M + Na]^+$: $C_{12}H_{11}NNaO$ 208.0733, found 208.0723.

Typical Procedure for Vinylsulfone Synthesis (Method A): To a solution of 1-[3-(benzo[*d*]thiazol-2-ylsulfonyl)propyl]-4,4-dimethylpiperidine-2,6-dione **2a** (300 mg, 0.79 mmol) in THF (24 mL) at –78 °C, was added boron trifluoride–diethyl ether (0.2 mL, 1.6 mmol) and lithium bis(trimethylsilyl)amide (1.0 M in toluene, 1.6 mL, 1.6 mmol). The mixture was stirred at –78 °C for 30 min. A phosphate buffer solution was added (3 mL) at –78 °C and the mixture was extracted three times with ethyl acetate. The combined organic layers were washed with brine, dried with Na_2SO_4 and the solvents evaporated under vacuum. The residue is dissolved in dry THF (24 mL) and $MgBr_2$ (291 mg, 1.58 mmol) was added. The mixture was stirred overnight at 50 °C. A phosphate buffer solution was added (3 mL) at –78 °C and the mixture was extracted three times with ethyl acetate. The combined organic layers were washed with brine, dried with Na_2SO_4 and the solvents evaporated under vacuum.

1-(Benzo[*d*]thiazol-2-ylsulfonyl)-7,7-dimethyl-2,6,7,8-tetrahydroindolizin-5-(3*H*)-one (4): The crude product was chromatographed on silica gel using petroleum ether/ethyl acetate (4:6) as eluent to afford pure compound **4** (261 mg, 92 %) as a white solid. ^{1}H NMR (300 MHz, $CDCl_3$): δ = 8.20–8.15 (m, 1 H), 8.01–7.96 (m, 1 H), 7.65–7.52 (m, 2 H), 3.94 (t, J = 9.0 Hz, 2 H), 3.07–2.94 (m, 4 H), 2.34 (s, 2 H), 1.06 (s, 6 H) ppm. ^{13}C NMR (75 MHz, $CDCl_3$): δ = 168.3, 167.5, 155.0, 153.0, 136.9, 127.9, 127.7, 125.5, 122.4, 113.0, 45.8, 44.4, 35.9, 31.4, 27.8, 27.2 ppm. IR: $\tilde{\nu}_{max}$ = 2954, 2948, 2925, 1680, 1602, 1465, 1389, 1339, 1321, 1291, 1281, 1274, 1149, 1106, 1083, 774, 732, 605 cm^{-1}. HRMS (ESI) calcd. for $[M + H]^+$: $C_{17}H_{19}N_2O_3S_2$ 363.0832, found 363.0822, m.p. 154–156 °C.

9-(Benzo[*d*]thiazol-2-ylsulfonyl)-2,2-dimethyl-1,2,3,6,7,8-hexahydro-4*H*-quinolizin-4-one (13): Evaporation gives pure compound **13** (300 mg, quant.) without further purification as a yellow-orange solid. ^{1}H NMR (300 MHz, $CDCl_3$): δ = 8.16 (d, J = 7.1 Hz, 1 H), 7.99 (d, J = 7.4 Hz, 1 H), 7.59 (m, 2 H), 3.76 (m, 2 H), 3.19 (s, 2 H), 2.72 (t, J = 6.2 Hz, 2 H), 2.40 (s, 2 H), 1.86 (m, 2 H), 0.98 (s, 6 H) ppm. ^{13}C NMR (75 MHz, $CDCl_3$): δ = 169.2, 168.3, 152.7, 150.6, 136.7, 127.8, 127.6, 125.3, 122.3, 114.5, 46.4, 40.8, 39.3, 29.7, 27.4, 25.4, 20.8 ppm. IR: $\tilde{\nu}_{max}$ = 2956, 2931, 2894, 2871, 1685, 1579, 1469, 1357, 1309, 1255, 1144, 1116, 762, 624 cm^{-1}. HRMS (ESI) calcd. for $[M + H]^+$: $C_{18}H_{21}N_2O_3S_2$ 377.0988, found 377.0994, m.p. 183–185 °C.

1-(Benzo[*d*]thiazol-2-ylsulfonyl)-9b-hydroxy-1,2,3,9b-tetrahydro-5*H*-pyrrolo[2,1-*a*]isoindol-5-one (19): Compound **19** was recovered as a white solid after dehydration in 47 % yield. ^{1}H NMR (400 MHz, [D$_6$]DMSO): δ = 8.34–8.28 (m, 1 H), 8.25–8.21 (m, 1 H), 7.98 (d, J = 7.6 Hz, 1 H), 7.75–7.56 (m, 5 H), 4.34 (dd, J = 11.2, 8.1 Hz, 1 H), 3.59 (m, 1 H), 3.48–3.42 (m, 1 H), 3.23–3.10 (m, 1 H), 2.72–2.61 (m, 1 H) ppm. ^{13}C NMR (101 MHz, [D$_6$]DMSO): δ = 168.4, 167.2, 152.3, 145.2, 136.5, 132.8, 131.7, 130.2, 128.2, 127.9, 125.2, 125.0, 123.4, 122.7, 94.8, 67.0, 39.5, 29.5 ppm. IR: $\tilde{\nu}_{max}$ = 3251, 2965, 2900, 1686, 1472, 1389, 1334, 1310, 1257, 1150, 1087, 761, 615, 522 cm^{-1}. HRMS (ESI) calcd. for $[M + Na]^+$: $C_{18}H_{14}N_2NaO_4S_2$ 409.0287, found 409.0285, m.p. 186–187 °C.

1-(Benzo[*d*]thiazol-2-ylsulfonyl)-10b-hydroxy-1,3,4,10b-tetrahydropyrido[2,1-*a*]isoindol-6(2*H*)-one (20): Compound **20** was recovered as a white solid after dehydration in 53 % yield. ^{1}H NMR (400 MHz, [D$_6$]DMSO): δ = 8.36–8.29 (m, 2 H), 8.27–8.20 (m, 1 H), 7.69 (m, 4 H), 7.61–7.55 (m, 1 H), 4.08–3.97 (m, 2 H), 2.92 (dd, J = 13.0, 9.8 Hz, 1 H), 2.46–2.39 (m, 1 H), 2.33–2.25 (m, 1 H), 1.85 (d, J = 12.3 Hz, 1 H), 1.56–1.40 (m, 1 H) ppm. ^{13}C NMR (101 MHz, [D$_6$]DMSO): δ = 166.3, 163.7, 152.2, 145.5, 136.5, 131.5, 131.3, 129.7, 128.2, 127.9, 126.7, 125.1, 123.4, 122.2, 86.5, 69.2, 34.7, 24.2, 23.2 ppm. IR: $\tilde{\nu}_{max}$ = 3221, 2944, 1670, 1473, 1416, 1317, 1148, 1020, 756, 727, 602, 577, 511 cm^{-1}. HRMS (ESI) calcd. for $[M + Na]^+$: $C_{19}H_{16}N_2NaO_4S_2$ 423.0444, found 423.0441, m.p. 211–213 °C.

Typical Procedure for Vinylsulfone Synthesis (Method B): To a solution of 1-[3-(benzo[*d*]thiazol-2-ylsulfonyl)propyl]-4,4-dimethylpiperidine-2,6-dione **2a** (300 mg, 0.79 mmol) in THF (24 mL) at –78 °C, was added boron trifluoride–diethyl ether (0.2 mL, 1.6 mmol) and lithium bis(trimethylsilyl)amide (1.0 M in toluene, 1.6 mL, 1.6 mmol). The mixture was stirred at –78 °C for 30 min. The reaction was quenched with acetyl chloride (115 µL, 1.6 mmol) at –78 °C. The reaction was warmed to room temperature and stirred for 12 h. A phosphate buffer solution was added (3 mL) at –78 °C and the mixture was extracted three times with ethyl acetate. The combined organic layers were washed with brine, dried with Na_2SO_4 and the solvents evaporated under vacuum. The crude product was chromatographed on silica gel using petroleum ether/EtOAc mixtures as eluent.

1-(Benzo[*d*]thiazol-2-ylsulfonyl)-2,6,7,8-tetrahydroindolizin-5-(3*H*)-one (14): The crude product was chromatographed on silica gel using 2:3 petroleum ether/EtOAc mixture as eluent to afford pure compound **14** (240 mg, 91 %) as a white-brown solid. ^{1}H NMR (300 MHz, $CDCl_3$): δ = 8.15 (d, J = 7.8 Hz, 1 H), 7.96 (d, J = 7.7 Hz, 1 H), 7.55 (m, 2 H), 3.90 (t, J = 9.5 Hz, 2 H), 3.09 (t, J = 6.0 Hz, 2 H), 2.97 (t, J = 9.4 Hz, 2 H), 2.47 (t, J = 6.3 Hz, 2 H), 1.91 (m, 2 H) ppm. ^{13}C NMR (75 MHz, $CDCl_3$): δ = 168.7, 167.4, 155.6, 152.9, 136.7, 127.8, 127.5, 125.4, 122.3, 111.6, 44.6, 32.0, 26.8, 22.8, 19.0 ppm. IR: $\tilde{\nu}_{max}$ = 2962, 2904, 2879, 2871, 1679, 1600, 1470, 1388, 1333, 1315, 1280, 1143, 1108, 763, 629 cm^{-1}. HRMS (ESI) calcd. for $[M + H]^+$: $C_{15}H_{15}N_2O_3S_2$ 335.0519, found 335.0525, m.p. 143–144 °C.

8-(Benzo[*d*]thiazol-2-ylsulfonyl)-1,5,6,7-tetrahydroindolizin-3-(2*H*)-one (15): The crude product was chromatographed on silica gel using petroleum ether/ethyl acetate mixture (4:6) as eluent to afford pure compound **15** (248 mg, 95 %) as a white-brown solid. ^{1}H NMR (300 MHz, $CDCl_3$): δ = 8.17 (dd, J = 7.5, 1.4 Hz, 1 H), 7.98 (dd, J = 7.3, 1.5 Hz, 1 H), 7.65–7.52 (m, 2 H), 3.53 (t, J = 5.9 Hz, 2 H), 3.50–3.42 (m, 2 H), 2.65–2.55 (m, 4 H), 1.87 (m, 2 H) ppm. ^{13}C NMR (101 MHz, $CDCl_3$): δ = 175.8, 168.1, 155.1, 153.0, 136.7, 127.7, 127.6, 125.4, 122.3, 106.4, 39.4, 28.0, 24.4, 23.0, 19.9 ppm. IR: $\tilde{\nu}_{max}$ = 2963, 2916, 2360, 2339, 1722, 1600, 1467, 1453, 1403, 1359, 1319, 1307, 1245, 1146, 1116, 1091, 1079, 1048, 1010, 991, 875, 850, 827, 807, 774, 631 cm^{-1}. HRMS (ESI) calcd. for $[M + Na]^+$: $C_{15}H_{14}N_2NaO_3S_2$ 357.0338, found 357.0341, m.p. 206–207 °C.

9-(Benzo[*d*]thiazol-2-ylsulfonyl)-1,2,3,6,7,8-hexahydro-4*H*-quinolizin-4-one (17): The crude product was chromatographed on silica gel using petroleum ether/ethyl acetate (4:6) as eluent to afford pure compound **17** (247 mg, 88 %) as an orange solid. ^{1}H NMR (300 MHz, $CDCl_3$): δ = 8.13 (dd, J = 7.4, 1.5 Hz, 1 H), 7.95 (dd, J = 7.3, 1.6 Hz, 1 H), 7.54 (m, 2 H), 3.70 (m, 2 H), 3.30 (t, J = 6.0 Hz, 2 H), 2.65 (t, J = 6.3 Hz, 2 H), 2.54 (t, J = 6.5 Hz, 2 H), 1.82 (m, 4 H) ppm. ^{13}C NMR (75 MHz, $CDCl_3$): δ = 169.7, 168.2, 152.7, 151.6, 136.6, 127.7, 127.4, 125.3, 122.2, 112.8, 41.0, 33.0, 26.7, 25.0, 20.6, 18.5 ppm. IR: $\tilde{\nu}_{max}$ = 2952, 2900, 2883, 1687, 1578, 1469, 1381, 1356, 1332, 1305, 1259, 1140, 1116, 1085, 1043, 766, 690, 628 cm^{-1}. HRMS

(ESI) calcd. for $[M + Na]^+$: $C_{16}H_{16}N_2NaO_3S_2$ 371.0495, found 371.0491, m.p. 85–86 °C.

Typical Procedure for Vinylsulfones Synthesis (Method C): To a solution of the sulfone **2g** (280 mg, 0.79 mmol) in THF (24 mL) at –78 °C, was added boron trifluoride–diethyl ether (0.2 mL, 1.6 mmol) and lithium bis(trimethylsilyl)amide (1.0 M in toluene) (1.6 mL, 1.6 mmol). The mixture was stirred at –78 °C for 30 min. A phosphate buffer solution was added (3 mL) at –78 °C and the mixture was extracted three times with ethyl acetate. The combined organic layers were washed with brine, dried with Na_2SO_4 and the solvents evaporated under vacuum. The residue is dissolved in dry DMF (1.6 mL) and methanesulfonyl chloride (67 µL, 0.868 mmol) was added at 0 °C, followed by the addition of triethylamine (0.13 mL, 0.947 mmol). The mixture was stirred at 90 °C for 12 h. Water was added at room temperature and the mixture was extracted three times with ethyl acetate. The combined organic layers were washed with water, then with brine, dried with Na_2SO_4 and the solvents evaporated under vacuum. The crude product was chromatographed on silica gel using petroleum ether/ethyl acetate mixtures as eluent.

4-(Benzo[*d*]thiazol-2-ylsulfonyl)-2,3,5,6-tetrahydro-7*H*-pyrrolo[1,2-*b*][1,2]oxazin-7-one (18): Compound **18** was prepared following Method C. The crude product was chromatographed on silica gel using petroleum ether/ethyl acetate (5:5) as eluent to afford pure compound **18** (190 mg, 71 %) as a brown solid. ^{1}H NMR (300 MHz, $CDCl_3$): δ = 8.16 (d, J = 8.2 Hz, 1 H), 7.98 (d, J = 7.6 Hz, 1 H), 7.58 (m, 2 H), 4.25 (t, J = 5.1 Hz, 2 H), 3.49–3.39 (m, 2 H), 2.84–2.76 (m, 2 H), 2.59 (m, 2 H) ppm. ^{13}C NMR (75 MHz, $CDCl_3$): δ = 167.3, 167.3, 152.9, 149.3, 136.7, 127.9, 127.7, 125.4, 122.3, 102.7, 68.9, 25.2, 23.6, 21.6 ppm. IR: $\tilde{\nu}_{max}$ = 2950, 2944, 2361, 2339, 1748, 1619, 1469, 1307, 1208, 1147, 1110, 1096, 1064, 982, 869, 850, 822, 763, 731, 690 cm^{-1}. HRMS (ESI) calcd. for $[M + H]^+$: $C_{14}H_{13}N_2O_4S_2$ 337.0311, found 337.0314, m.p. 161–162 °C.

1-(Benzo[*d*]thiazol-2-ylsulfonyl)-2,3-dihydro-5*H*-pyrrolo[2,1-*a*]-isoindol-5-one (21): Compound **21** was prepared following Method C. The crude product was chromatographed on silica gel using petroleum ether/ethyl acetate (7:3) as eluent to afford pure compound **21** (156 mg, 54 %) as a yellow solid. ^{1}H NMR (400 MHz, $CDCl_3$): δ = 8.66 (d, J = 7.6 Hz, 1 H), 8.18 (d, J = 6.0 Hz, 1 H), 7.97 (d, J = 6.0 Hz, 1 H), 7.81 (d, J = 6.9 Hz, 1 H), 7.68 (m, 2 H), 7.58 (m, 2 H), 4.01 (t, J = 8.6 Hz, 2 H), 3.61 (t, J = 8.6 Hz, 2 H) ppm. ^{13}C NMR (101 MHz, $CDCl_3$): δ = 166.5, 163.9, 153.1, 151.1, 136.9, 135.9, 132.8, 132.7, 128.2, 128.2, 127.8, 127.7, 125.7, 123.8, 122.4, 113.3, 40.4, 34.7 ppm. IR: $\tilde{\nu}_{max}$ = 2920, 2861, 1715, 1623, 1467, 1393, 1352, 1331, 1144, 1093, 769, 690, 618, 567 cm^{-1}. HRMS (ESI) calcd. for $[M + H]^+$: $C_{18}H_{13}N_2O_3S_2$ 369.0362, found 369.0352, m.p. 215–217 °C.

1-(Benzo[*d*]thiazol-2-ylsulfonyl)-3,4-dihydropyrido[2,1-*a*]isoindol-6(2*H*)-one (22): Compound **22** was prepared following Method C. The crude product was chromatographed on silica gel using petroleum ether/ethyl acetate (7:3) as eluent to afford pure compound **22** (144 mg, 47 %) as a yellow solid. ^{1}H NMR (400 MHz, $CDCl_3$): δ = 9.02 (d, J = 8.0 Hz, 1 H), 8.14–8.09 (m, 1 H), 8.00–7.94 (m, 1 H), 7.83 (d, J = 6.9 Hz, 1 H), 7.67 (m, 1 H), 7.62–7.51 (m, 3 H), 3.83–3.78 (m, 2 H), 3.03 (t, J = 6.2 Hz, 2 H), 2.05 (d, J = 6.1 Hz, 2 H) ppm. ^{13}C NMR (101 MHz, $CDCl_3$): δ = 166.9, 166.1, 152.4, 144.9, 136.5, 132.8, 132.0, 131.4, 129.8, 128.6, 127.9, 127.5, 125.4, 123.0, 122.2, 115.2, 38.5, 26.4, 20.6 ppm. IR: $\tilde{\nu}_{max}$ = 2925, 2853, 1715, 1587, 1468, 1394, 1367, 1321, 1298, 1143, 1084, 1013, 765, 696, 615 cm^{-1}. HRMS (ESI) calcd. for $[M + Na]^+$: $C_{19}H_{14}N_2NaO_3S_2$ 405.0322, found 405.0338, m.p. 140–142 °C.

Acknowledgments

Financial support from the Ministère de l'Enseignement Supérieur et de la Recherche (Research Fellowship for HVT), France is gratefully acknowledged. L. P. thanks the CCIR of ICBMS and the P2CHPD (Université Claude Bernard Lyon 1) for the generous allocation of computational resources and technical support.

Keywords: Synthetic methods · Olefination · Imides · Lactams · Molecular modeling

[1] J. W. Daly, *J. Nat. Prod.* **1998**, *61*, 162–172.
[2] J. P. Michael, *Nat. Prod. Rep.* **2008**, *25*, 139–165.
[3] V. D. Chaudhari, K. S. A. Kumar, D. D. Dhavale, *Tetrahedron* **2006**, *62*, 4349–4354.
[4] See, for example: T. Tite, F. Jacquelin, L. Bischoff, C. Fruit, F. Marsais, *Tetrahedron: Asymmetry* **2010**, *21*, 2032–2036.
[5] For a recent example, see: A. Rajender, J. P. Rao, B. V. Rao, *Eur. J. Org. Chem.* **2013**, 1749–1757.
[6] See, for example: G. Lapointe, K. Schenk, P. Renaud, *Chem. Eur. J.* **2011**, *17*, 3207–3212.
[7] See, for example: T. Ayad, Y. Genisson, M. Baltas, L. Gorrichon, *Chem. Commun.* **2003**, 582–583.
[8] See, for example: X. Q. Tang, J. Montgomery, *J. Am. Chem. Soc.* **1999**, *121*, 6098–6099.
[9] *The Logic of Chemical Synthesis* (Eds.: E. J. Corey, X.-M. Cheng), John Wiley & Sons, New York, **1989**.
[10] T. Taniguchi, H. Ishibashi, *Heterocycles* **2013**, *87*, 527–545.
[11] D. C. Ha, C. S. Yun, E. Yu, *Tetrahedron Lett.* **1996**, *37*, 2577–2580.
[12] A. G. Griesbeck, N. Hoffmann, K. D. Warzecha, *Acc. Chem. Res.* **2007**, *40*, 128–140.
[13] S. Santra, N. Masalov, O. L. Epstein, J. K. Cha, *Org. Lett.* **2005**, *7*, 5901–5904.
[14] N. Kise, Y. Inoue, T. Sakurai, *Tetrahedron Lett.* **2013**, *54*, 3281–3285.
[15] a) J. B. Baudin, G. Hareau, S. A. Julia, O. Ruel, *Tetrahedron Lett.* **1991**, *32*, 1175–1178; b) J. B. Baudin, G. Hareau, S. A. Julia, R. Lorne, O. Ruel, *Bull. Soc. Chim. Fr.* **1993**, *130*, 856–878; c) P. R. Blakemore, *J. Chem. Soc. Perkin Trans. 1* **2002**, *23*, 2563–2585.
[16] a) D. Gueyrard, R. Haddoub, A. Salem, N. Said Bacar, P. G. Goekjian, *Synlett* **2005**, 520–522; b) B. Bourdon, M. Corbet, P. Fontaine, P. G. Goekjian, D. Gueyrard, *Tetrahedron Lett.* **2008**, *49*, 747–749; c) S. Habib, F. Larnaud, E. Pfund, T. Lequeux, B. Fenet, P. G. Goekjian, D. Gueyrard, *Eur. J. Org. Chem.* **2013**, 1872–1875; d) S. Habib, D. Gueyrard, *Eur. J. Org. Chem.* **2015**, 871–875.
[17] N. Gigant, S. Habib, M. Medoc, P. G. Goekjian, D. Gueyrard, I. Gillaizeau, *Eur. J. Org. Chem.* **2014**, 6501–6506.
[18] a) C. Aissa, *J. Org. Chem.* **2006**, *71*, 360–363; b) P. Jakubec, D. M. Cockfield, D. Dixon, *J. Am. Chem. Soc.* **2009**, *131*, 16632–16633; c) H. E. Giesbrecht, B. J. Knight, N. R. Tanguileg, C. R. Emerson, P. R. Blakemore, *Synlett* **2010**, 374–378; d) Y. Zhao, B. Gao, C. Ni, J. Hu, *Org. Lett.* **2012**, *14*, 6080–6083; e) E. Rodrigo, J. L. Garcia Ruano, M. Belen Cid, *J. Org. Chem.* **2013**, *78*, 10737–10746.
[19] S. Du-A-Man, D. Soorukram, C. Kuhakarn, P. Tuchinda, V. Reutrakul, M. Pohmakotr, *Eur. J. Org. Chem.* **2014**, 1708–1715.
[20] L. Legnani, A. Porta, P. Caramella, L. Toma, G. Zanoni, G. Vidari, *J. Org. Chem.* **2015**, *80*, 3092–3100.
[21] R. Robiette, J. Pospisil, *Eur. J. Org. Chem.* **2013**, 836–840.
[22] Calculations were performed using the M06-2X meta-GGA functional. All atoms have been represented by the all electron triple-ζ 6-311G(*d*,*p*) basis sets. Bulk solvation by THF has been taken into during the optimization and frequency calculations using the SMD model. The detailed computational procedure is available as a supporting material.
[23] For the 1,3-diketo analog, conformational sampling has been limited to the formation of a *trans*-decalin structure. Barriers for ring closing in the *cis*-decalin structures were much higher (12.7 and 10.8 kcal mol^{-1} for *syn*- and *anti*-additions) due to 1,3-diaxial interactions.
[24] R. T. Watson, V. K. Gore, K. R. Chandupatla, R. K. Dieter, J. P. Snyder, *J. Org. Chem.* **2004**, *69*, 6105–6114.

[25] M. Corbet, B. Bourdon, D. Gueyrard, P. G. Goekjian, *Tetrahedron Lett.* **2008**, *49*, 750–754.
[26] Experimental procedures, spectroscopic data and copies of the ^{1}H and ^{13}C NMR spectra for compounds **2a**–**i** are available in the Supporting Information.
[27] A radical mechanism was further confirmed by the observation that the reaction did not take place, in: the presence of a radical inhibitor (BHT). Additional studies will be reported, in: due course, but this side reaction may be relevant for other studies of heteroarylsulfones at high temperatures.
[28] Experimental procedures, spectroscopic data and copies of the ^{1}H NMR spectrum of the sulfone-THF coupling compound are available in the Supporting Information.
[29] The addition step mediated by LiHMDS has been monitored by in situ FTIR (reactIR). It confirms the quantitative conversion of the starting material into hemiaminals. No starting material was observed after low temperature quench. Similar studies of the elimination step were inconclusive due to overlap by the IR signals of the DBU. See Supplementary information.
[30] a) S. Luo, Y. Zhao, D. G. Truhlar, *Phys. Chem. Chem. Phys.* **2011**, *13*, 13683–13689; b) Y. Zhao, D. G. Truhlar, *J. Chem. Theory Comput.* **2008**, *4*, 1849–1868.
[31] An alternative interpretation would be that the dimethyl group rigidifies the ring system. However, molecular dynamics simulations did not show a significant difference in the amplitude of the variation in the S–H_{ax} distance. The more significant effect was on the average distance: 2.78 Å for the dimethyl case versus 2.85 Å in the unsubstituted case, see the Supporting Information.

Received: March 21, 2016
Published Online: June 8, 2016

